Journal of Biomedical Optics

SPIEDigitalLibrary.org/jbo

Choosing optimal wavelength for photodynamic therapy of port wine stains by mathematic simulation

Ying Wang
Ying Gu
Zhaohui Zuo
Naiyan Huang

SPIE

Choosing optimal wavelength for photodynamic therapy of port wine stains by mathematic simulation

Ying Wang, Ying Gu, Zhaohui Zuo, and Naiyan Huang
Chinese People's Liberation Army General Hospital, Department of Laser Medicine, Beijing 100853, China

Abstract. Many laser wavelengths have been used in photodynamic therapy (PDT) for port wine stains (PWS). However, how these wavelengths result in different PDT outcomes has not been clearly illuminated. This study is designed to analyze which wavelengths would be the most advantageous for use in PDT for PWS. The singlet oxygen yield in PDT-treated PWS skin under different wavelengths at the same photosensitizer dosage was simulated and the following three situations were simulated and compared: 1. PDT efficiency of 488, 532, 510, 578, and 630 nm laser irradiation at clinical dosage (100 mW/cm^2, 40 min); 2. PDT efficiency of different wavelength for PWS with hyperpigmentation after previous PDT; 3. PDT efficiency of different wavelengths for PWS, in which only deeply located ectatic vessels remained. The results showed that singlet oxygen yield is the highest at 510 nm, it is similar at 532 nm and 488 nm, and very low at 578 nm and 630 nm. This result is identical to the state in clinic. According to this theoretical study, the optimal wavelength for PDT in the treatment of PWS should near the absorption peaks of photosensitizer and where absorption from native chromophores (haemoglobin and melanin) is diminished. [DOI: 10.1117/1.3616127]

Keywords: mathematic simulation; photodynamic therapy; port wine stain; singlet oxygen yield.

Paper 11138RR received Mar. 23, 2011; revised manuscript received Jul. 2, 2011; accepted for publication Jul. 7, 2011; published online Sep. 1, 2011; corrected Sep. 27, 2011.

1 Introduction

Port wine stain (PWS) is a congenital birthmark histologically characterized by ectatic vessels within the papillary and reticular dermis.[1] The goal of treatment is to clear the red color of PWS by selectively destroying the ectatic blood vessels without damaging the normal epidermis and dermis. In 1983, Anderson and Parrish[2] proposed the theory of selective photothermolysis. Since then, pulsed dye laser was used in the treatment of PWS. However, it is not able to clear the red color for most PWS patients and has the risk of inducing thermal damage to normal epidermis,[3] especially for individuals with highly pigmented skin.

In 1991, Gu et al. successfully applied vascular targeted photodynamic therapy (V-PDT) to the treatment of PWS.[4] The selective destruction of V-PDT to the ectatic blood vessels in PWS is obtained by two factors. One is selective distribution of photosensitizer in vessels instead of normal epidermis and deep dermis short time after intravenous injection of photosensitizer. Different from PDT for tumors, laser irradiation starts immediately after photosensitizer injection in V-PDT for PWS, which can provide a maximum amount of photosensitizer in the vasculature as opposed to the surrounding tissue. Then, a selective destruction of ectatic vessels in PWS can be obtained. The other is selective distribution of laser in the superficial layer of skin at a certain short wavelength (e.g., 488 or 532 nm), which can only penetrate to the superficial dermis of PWS skin. Though, theoretically, with short laser wavelength, there is still little amount light distributed in deep dermis. But the intensity of light is too low to generate PDT damage to dermis. Moreover, the power intensity of laser irradiation is much lower than PDL (only 80 or 100 mW/cm^2). No thermal damage could occur to normal epidermis. Therefore, PDT reaction can only occur in the superficial vessels where photosensitizer and light are simultaneously present. In normal epidermis and deep dermis, no PDT reaction would occur since photosensitizer or laser light is absent.[5] In clinic, PWS patients usually need multiple treatments to clear all the ectatic blood vessels, as the vessels are damaged layer by layer in V-PDT.

V-PDT dosage includes light dosage, photosensitizer dosage, and oxygen content. Oxygen content in the target tissue is an important factor influencing the treatment result for tumor. However for PWS, the oxygen content decreases only in those PWS with purple color or hyperplastic nodules. Preliminary experiments showed that the oxygen content change in this situation did not influence the PDT outcome of PWS.[6] Therefore, the distribution of light and photosensitizer in target tissue are the main factors determining the final treatment efficacy for PWS. The photosensitizer content in PWS skin can be monitored *in vivo* using fluorescence spectra and the administration dosage can be adjusted in the following treatment.[7] Hence, the choice of optimal wavelength has been extensively studied.

In clinic, an Ar ion (488 nm) laser combined with the first generation photosensitizer (HpD) was first used in PDT for PWS. Then, KTP (potassium titanyl phosphate, 532 nm) laser and Hematoporphyrin monomethyl ether (HMME) were applied to clinic. Early clinical work showed that V-PDT could gain good therapeutic outcome in lesions resistant to PDL.[8] Therefore, this technique was rapidly adopted. In the following years, copper vapor laser (510.6 and 578.2 nm) was applied in PDT for PWS with good treatment result.[9] However, copper vapor laser is large and needs cooling by a circulating water system. Moreover, the

Address all correspondence to: Ying Gu, The PLA General Hospital, The Department of Laser Medicine, 28 Fuxing Road, Beijing 100853, China. Tel: 86 10–66939394; E-mail: guyinglaser@sohu.com.

1083-3668/2011/16(9)/098001/8/$25.00 © 2011 SPIE

operation procedure is tedious. All of these factors hindered the use of copper vapor laser.

Though there are many wavelengths (such as 413, 488, 532, 510, and 578 nm) available for PWS PDT treatment, clinically, it is not easy to choose a suitable laser for different types of PWS. The excitation efficiency and distribution feature of light in PWS skin at each wavelength are different, because the age, skin color, and morphosis of PWS has significant influence on light distribution at different wavelengths. The mechanism how these differences result in the different PDT outcomes has not been illuminated. Therefore, a mathematical model simulating the complex PDT process is useful to enhance our understanding of the fundamental processes in PDT and improve the clinical treatment efficacy. In the present study, we simulated the singlet oxygen yield in PDT-treated PWS skin under a different wavelength at the same photosensitizer dosage using a mathematical model previously established.[10] Different types of PWS were modeled by changing the depth of vessels and the melanin content in the epidermis. The singlet oxygen yield in the target PWS vessels was compared, then a potential individualized PDT light dosage was proposed.

2 Materials and Methods

2.1 *Mathematical Model*

A singlet oxygen-mediated (Type II reaction) PDT reaction was simulated to analyze the singlet oxygen yield in PWS tissue under five wavelengths (488, 532, 510, 578, and 630 nm). This mathematical model is composed of four sub-models: light deposition simulation, oxygen diffusion, photosensitizer diffusion, and singlet oxygen generation. The interrelationship between light, oxygen, and photosensitizer was illustrated in Fig. 1.

Photosensitizer is administered to vessels by intravenous injection, and laser irradiation starts immediately after photosensitizer injection. The concentration of photosensitizer changes due to metabolism in vessels. The light deposited in target vessels can excite the photosensitizer in vessels to start a series of photochemical reactions. The energy of excited photosensitizer is transferred to oxygen and singlet oxygen is generated. Then, singlet oxygen reacts with biomolecules to initiate the blocking of target vessels. As a concomitant reaction, part of the photosensitizer can be photobleached by singlet oxygen.

Using this model, the following three situations were simulated and analyzed: 1. compare the efficacy of PDT under 488, 532, 510, 578, and 630 nm laser irradiation, at the clinical light dosage (irradiated for 40 min under the power density of 100 mW/cm^2); 2. compare the efficacy of different wavelength PDT for PWS with hyperpigmentation after previous PDT; 3. compare the efficacy of different wavelength PDT for PWS in which only deeply located ectatic vessels remained after several PDT courses.

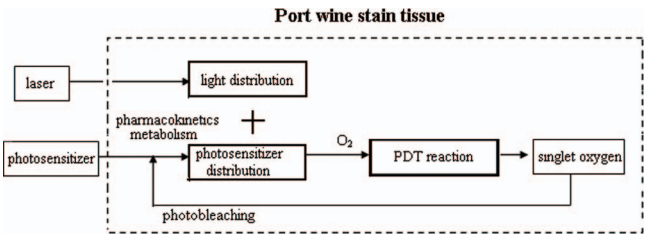

Fig. 1 Block diagram of PDT reaction in port wine stains.

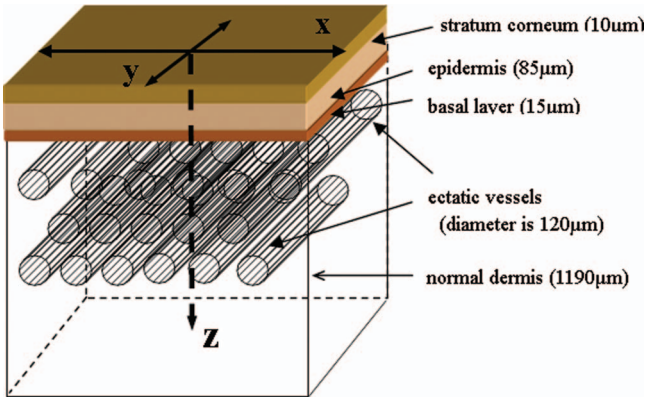

Fig. 2 Geometry model of PWS skin with ectatic vessels. It consists of stratum corneum, epidermis (with less melanin, m% = 0.1%) above the basal melanin layer, basal melanin layer (contains a lot of melanin), and dermis embedded with three layers ectatic vessels.

2.2 *Light Deposition Simulation*

Monte Carlo based method was used to calculate the light energy deposition in PWS skin.

2.2.1 *Port wine stains skin geometry*

The PWS skin geometry used in our modeling was previously described.[11] It consists of stratum corneum, epidermis above the basal melanin layer, basal melanin layer, and dermis embedded with three-layer ectatic vessels (Fig. 2). The vertical separation between two layers and the lateral separation between two capillaries were 20 μm. The capillary depth (separation between epidermal-dermal junction and the up wall of the first layer capillary) was set at 100 μm. The total thickness of skin is 13,000 μm, not including the subcutaneous tissue below the dermis. The total epidermis melanin content (m%) was set at 2% for PWS without hyperpigmentation and 6% for PWS with hyperpigmentation. The vessels are parallel to the Y axis. The laser beam diameter is 1 mm at $x, y = 0$ μm.

2.2.2 *Optical properties of port wine stains skin*

In literature, the optical parameters of epidermis or dermis usually lack a detailed description of melanin content or blood content. In this study, the skin optical properties at different wavelengths were determined by calculations based on the optical property parameters of melanin, blood (hemoglobin), melanin-less epidermis, bloodless dermis, and the volume fraction of each component (Fig. 3 and 4). The parameters at five wavelengths (488, 532, 510, 578, and 630 nm) were calculated according to the method used in previous study.[12] The parameters were listed in Table 1. The calculation process is described in the Appendix.

2.2.3 *Monte Carlo modeling of light deposition*

Our Monte Carlo algorithm was implemented under the following assumptions: for semi-infinite tissue sample, upper boundary

Table 1 Human skin optical properties used in the present study. SC: stratum corneum, the unit of μ_a and μ_s is cm^{-1}, m%: the percentage content of melanin in the whole epidermis.

			Epidermis		Dermis	
Wavelength (nm)	Optical properties	SC	Epidermis with 0.1% melanin	Basal layer	Dermis without ectatic vessels	Blood (hemoglobin)
488	μ_a	193	1.5	44.3 (m% = 2%)	1.9	112.7
	μ_s	2200	223.3	223.3	223.3	500
	g	0.915	0.762	0.762	0.762	0.98
	n	1.45	1.4	1.4	1.4	1.33
	μ_a	187	1.27	38.7 (m% = 2%)	1.8	112.5
510				115 (m% = 6%)		
	μ_s	2200	202.2	202.2	202.2	500
	g	0.920	0.768	0.768	0.768	0.980
	n	1.45	1.4	1.4	1.4	1.33
	μ_a	181	1.1	34 (m% = 2%)	2.6	206.2
532				101 (m% = 6%)		
	μ_s	2200	184.4	184.47	184.4	500
	g	0.925	0.774	0.774	0.774	0.980
	n	1.45	1.4	1.4	1.4	1.33
	μ_a	166	0.79	25 (m% = 2%)	2.8	240.9
578	μ_s	2200	151	151	151	500
	g	0.938	0.788	0.788	0.788	0.980
	n	1.45	1.4	1.4	1.4	1.33
	μ_a	151	0.62	19.2	0.4	9.86
630	μ_s	2200	129	129	129	500
	g	0.955	0.803	0.803	0.803	0.980
	n	1.45	1.4	1.4	1.4	1.33

Table 2 Main parameters and references.

Symbol	Meaning	Unit	Value	Reference
D_m	diffusion coefficient of photosensitizer	$\mu m^2/s$	50	13
D_s	diffusion coefficient of oxygen	$\mu m^2/s$	1500	14
k_P/k_{ot}	ratio between k_P and k_{ot}	mol/L	2.5	15
Γ_1	metabolic consumption of oxygen	$\mu M/s$	1.7	16
Φ	quantum yield of singlet oxygen yield		0.6	17

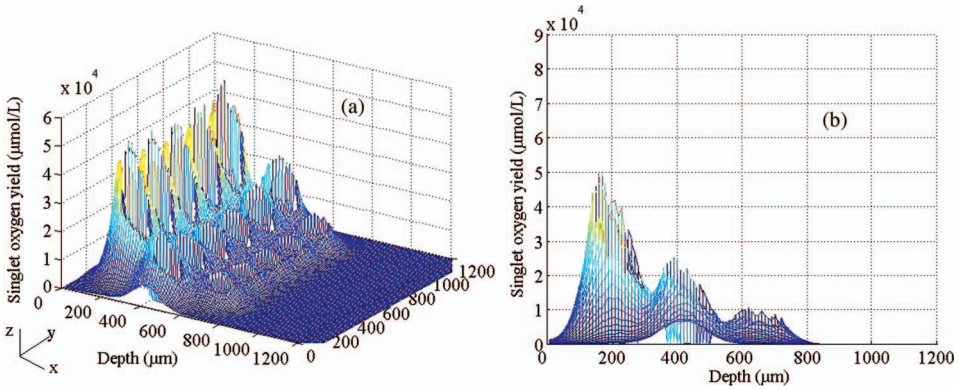

Fig. 3 Spatial profiles of singlet oxygen yield of 532 nm PDT in PWS tissue model.

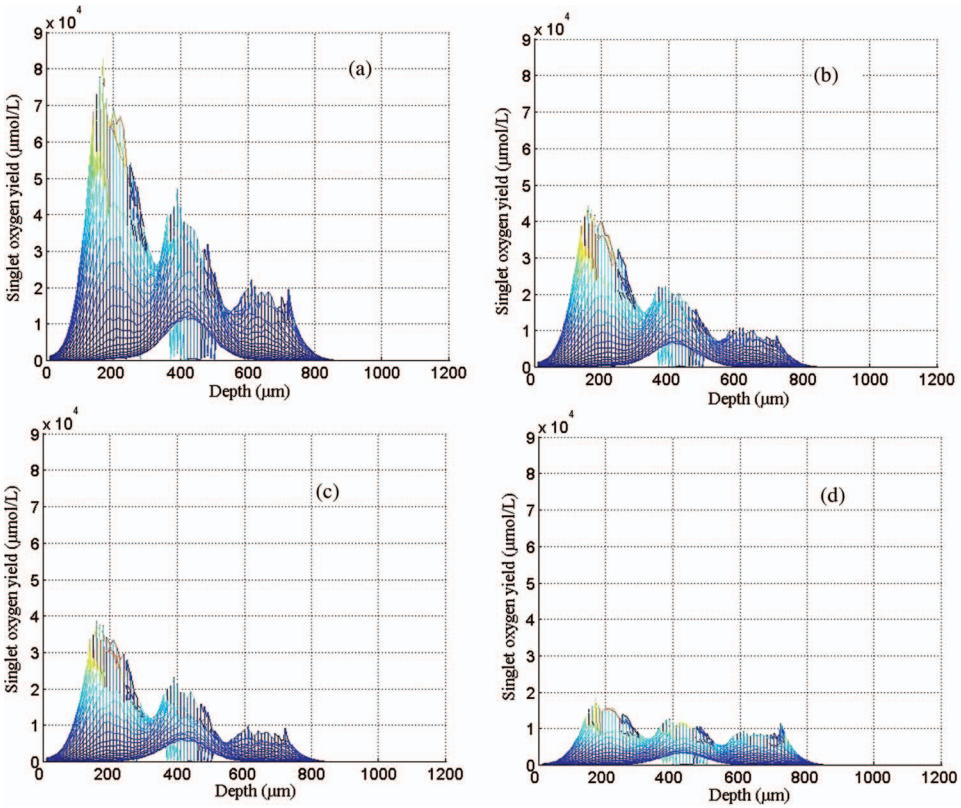

Fig. 4 Depth profiles of singlet oxygen yield in PWS tissue model at four other wavelengths: (a) 510, (b) 488, (c) 578, and (d) 630 nm.

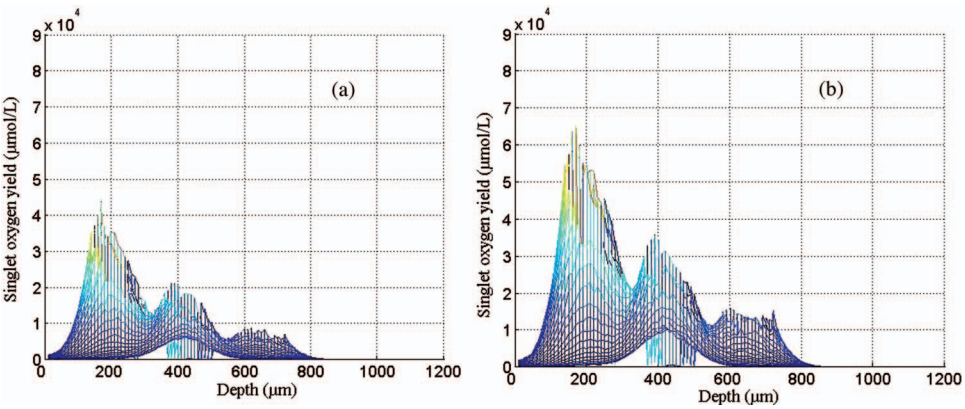

Fig. 5 Depth profiles of singlet oxygen yield in PWS with hyperpigmentation (melanin content in epidermis is 6%). [(a) is 532 nm and (b) is 510 nm; both are under the same power density and irradiation time.]

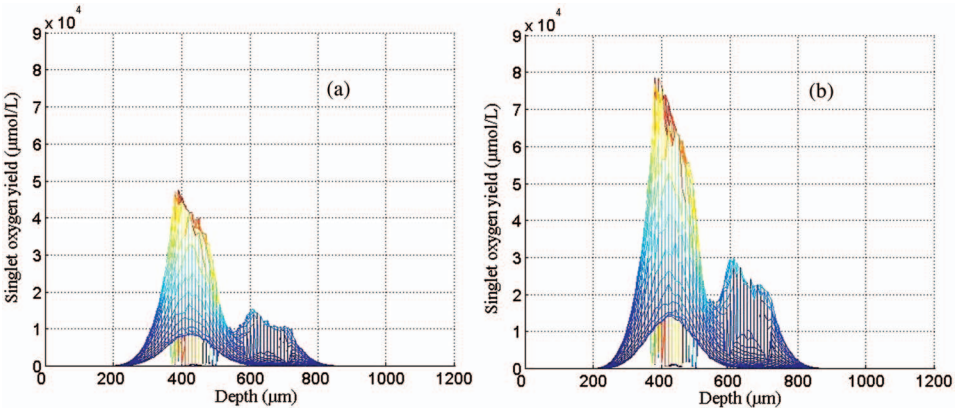

Fig. 6 The singlet oxygen yield in PWS in which the first layer vessels have been cleared in the previous treatments [(a) 532 and (b) 510 nm; both are under the same power density and irradiation time].

condition meets Neumann condition $\nabla u = 0$, lower boundary condition at the infinite depth meets Dirichlet condition $u = 0$, and the whole system is eudipleural. Three-dimensional Cartesian coordinate system (x, y, z) was established on the tissue sample, and the z-axis is normal to the tissue surface pointing toward the inside of the tissue. A three-dimensional homogeneous grid system was also set up in x,y,z directions. The grid line separations are dx = dy = dy = 5 μm with total numbers of grid elements Nx = Ny = Nz = 250. A pencil beam with radiant exposure of 240 J/cm^2 (100 mW/cm^2 × 40 min) is incident along the z-axis.

2.3 *Oxygen Content in Vessel and Tissue*

As in PWS, oxygen is diffused from vessels to the surrounding tissue. It is assumed that the oxygen content is high and constant in vessels, and the oxygen content in tissue was presented as the following equation:

$$D_s \cdot \nabla^2 C_O - \frac{\partial C_O}{\partial t} = \Gamma_1 + \Gamma_2, \tag{1}$$

where C_O is oxygen content, D_S is diffusion coefficient of oxygen, Γ_1 is metabolism consumption of oxygen, and Γ_2 is PDT consumption of oxygen.

2.4 *Photosensitizer Content in Vessel and Tissue*

Photosensitizer (Hematoporphyrin monomethyl ether, HMME) content in vessels was calculated according to the pharmacokinetics Eq. (2) measured in animals (unpublished data), as there is no data for humans. We set the same photosensitizer dosage for each wavelength. This would not affect the comparison results between different wavelengths by using the pharmacokinetics equation of photosensitizer for animals or for humans

$$C = 265.97e^{-0.376t} + 3.67e^{-0.034t} + 0.79e^{-0.004t}. \tag{2}$$

As in PWS, photosensitizer is also diffused from vessels to the surrounding tissue and can be photobleached by singlet oxygen during PDT. Therefore, photosensitizer content in tissue can be expressed

$$D_m \cdot \nabla^2 C_m - \frac{\partial C_m}{\partial t} = \Gamma_{PDT}, \tag{3}$$

where C_m is the concentration of photosensitier (mol/L), D_m is the diffusion coefficient of photosensitizer, and Γ_{PDT} is the photobleaching consumption of photosensitizer.

2.5 *Calculation of Singlet Oxygen Yield*

According to the principle of photochemical reaction, singlet oxygen yield can be calculated

$$\phi_{^1O_2} = \phi_\Delta \cdot I, \tag{4}$$

where $\phi_{^1O_2}$ is the productivity of singlet oxygen, ϕ_Δ is singlet oxygen quantum yield of HMME, and I is the light absorbed by photosensitizer in the target tissue and calculated as the following according to the Lambert-Beer's law,

$$I = I_0(\lambda) \cdot \varepsilon(\lambda) \cdot c, \tag{5}$$

where I_0 is the fluence rate of light deposited in the target tissue obtained from Monte Carlo modeling, $\varepsilon(\lambda)$ is the molar extinction coefficient of HMME at a certain wavelength, and C is the concentration of HMME. Then, the singlet oxygen yield can be

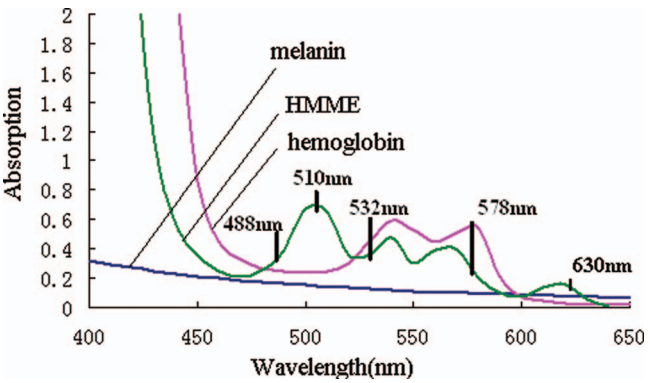

Fig. 7 Absorption spectra of melanin, hemoglobin, and HMME. The data of melanin and hemoglobin in water was cited from Ref. 20, the spectra of HMME was measured in albumin buffer.

expressed as

$$\phi_{^1O_2}(\lambda, z) = \phi_\Delta \cdot I_0(\lambda, z) \cdot \varepsilon(\lambda) \cdot c. \quad (6)$$

The photosensitizer and oxygen concentrations in each tissue unit at each time point can be calculated according to Eqs. (1)–(3). The light intensity in each tissue unit can be modeled by the Monte Carlo algorithm. Therefore, the total yield of singlet oxygen can be obtained by the numerical integration according to the following equation:

$$\Pi_{^1O_2}(t) = \Phi \cdot I \cdot [1 - \exp(-2.303\varepsilon \cdot C_m(t) \cdot l)] \times \frac{[^3O_2](t)}{[^3O_2](t) + k_p/k_{ot}}/V, \quad (7)$$

where $\prod^1{}_{O2}$ (t) is singlet oxygen yield (mol/L · s), I is the power of laser (mol/s, presented by the amount of optical photon), l is light path (cm), V is volume (L). When $V \to 0$, $\prod^1{}_{O2}$ (t) represents the singlet oxygen yield of certain position in tissue. $[^3O_2]$ is the concentration of O_2 (μM/L), k_P is the self-quench rate constant of triplet state oxygen, k_{ot} is the rate constant of triplet state photosensitizer quenched by O_2 (Table 2).

2.6 *Molar Extinction Coefficient of Hematoporphyrin Monomethyl Ether*

As there was no data about the molar extinction coefficient of HMME, experiment was done to calculate the molar extinction coefficient of HMME in albumin buffer. The molar extinction coefficients at these five wavelengths were calculated according to the Lambert-Beer law ($A = \epsilon l$), by measuring the absorption rate of HMME solutions at a series of concentration (2, 10, 20, 40, 60, 80, and 100 μmol/L).

A is the absorptance value,$\epsilon$is the molar extinction coefficient, and l is the light path (i.e., the width of the cuvette used in our measurement is 0.1 cm).

3 Results

3.1 *Molar Extinction Coefficient of Hematoporphyrin Monomethyl Ether in Albumin Buffer*

The measured molar extinction coefficients of HMME in albumin buffer were listed in Table 3. The coefficient at 510 nm is the largest, while the lowest is at 578 nm. The coefficient at 532 nm is similar to that at 488 nm (Table 3).

Table 3 Molar extinction coefficient of HMME in albumin buffer.

Wavelength (nm)	510	532	488	578	630
Molar extinction coefficient (L/mol.cm)	14600	9252	8960	6403	1962

3.2 *Singlet Oxygen Yield of Photodynamic Therapy in Port Wine Stains Tissue Under Different Wavelengths*

The simulation results showed that singlet oxygen was distributed mainly in the area near the vessel wall. In the vessels, the singlet oxygen yield close to the upper wall is higher than that at the bottom wall, and even higher than that in the center. The singlet oxygen yield in the first layer vessels is higher than those in the second and third layer vessels. The distribution trend of singlet oxygen yield in PWS tissue is similar under the five wavelengths.

As compared to 532 nm, which is commonly used in clinic, the singlet oxygen yield at 510 nm is the highest. Singlet oxygen yield at 532 nm is similar to that at 488 nm, while those at 578 and 630 nm are very low.

Singlet oxygen was distributed mainly in the area near the vessel walls. In the vessels, the singlet oxygen yield close to the upper wall is higher than that in the bottom wall. Nearly no singlet oxygen is generated at the center of the vessels. The singlet oxygen yield in the first layer vessels is higher than those in the second and third layer vessels.

3.3 *Modeling Results of Singlet Oxygen Yield in Port Wine Stains with Hyperpigmentation after Photodynamic Therapy*

For 532 nm, the singlet oxygen yield in the first layer vessels is about 4×10^4 μmol/L when the melanin content is 2%. It decreases to about 3×10^4 μmol/L (about 25%) when the melanin content increases to 6%. Meanwhile, for 510 nm, the singlet oxygen yield in the first layer vessels also decreases about 25%, however, still higher than 4×10^4 μmol/L (the level of singlet oxygen yield at 532 nm in PWS with 2% melanin content) (see Fig. 5).

3.4 *Modeling Results of Singlet Oxygen Yield in Port Wine Stains that have been Treated with Photodynamic Therapy for Several Courses*

After the first layer vessels are cleared, the singlet oxygen yield in superficial layer vessels (the previous second layer vessels) increases at both 532 and 510 nm. The total singlet oxygen yield in the present first layer vessels at 510 nm is higher than that at 532 nm (see Fig. 6).

4 Discussions

V-PDT is a promising treatment technique developed in the recent twenty years characterized by highly targeting and precise selective destruction to the lesion vessels. It is applicable to various types PWS, especially for PWS in yellow race. As the power intensity of laser used in PDT is much lower than PDL (only 80 or 100 mW/cm^2), no thermal damage could occur to normal epidermis. In clinical practice, it is a relatively safe treatment technique with less adverse effect, such as hyperpigmentation. But, the doctor must be well trained and have good knowledge of this technique. The use of an inappropriate laser wavelength or inappropriate irradiation time may lead to scars by damaging the surrounding and deep normal dermis. Since V-PDT was

applied in the treatment of PWS, the choice of laser wavelength has long been an important work in the individualization of PDT dosimetry. In 1997, Gu et al. carried out an *in vivo* experiment using comb as animal model for PWS to systematically compare the PDT reaction severity (blanching effect) and the feature of tissue damage at different laser wavelengths. The results are identical to our present simulation study. The experimental results showed that PDT at 510.6, 488, and 578.2 nm can lead to selective blocking of vessels in the superficial dermis, and no damage to normal epidermis and deep dermis was observed. PDT reaction at 510.6 nm was more severe compared to 488 and 578.2 nm. While the blanching effect of 627.8 nm was very poor, damage of the epidermis and deep dermis was observed at this wavelength. At that time, the reason that 510 nm laser had an excellent blanching effect was attributed to selective absorption of 510 nm laser by haemoglobin and a deeper penetration than 488 and 532 nm.[9] As the backscattering of 630 nm wavelength in skin is less than 488, 510, and 578 nm, it can penetrate skin deeper than other wavelengths. In addition, the extinction coefficient of HMME at 630 nm is lower than those at other wavelengths. As a result, the PDT reaction mediated by 630 nm in PWS skin is poor and has a lack of selectivity.

With the theoretical analysis in this study, we have a new explanation of the reason that 510 nm has an excellent blanching effect. It is attributed to two factors: one is that the extinction coefficient of HMME at 510 nm is the largest among these wavelengths. The other is that 510 nm laser intensity deposited in PWS vessels is higher than all other wavelengths. This is because less than 510 nm laser is absorbed by hemoglobin in PWS vessels, as 510 nm locates in the low ebb of hemoglobin absorption spectra (Fig. 7).

In the early stage of the studies for wavelength choice for PDT, the laser wavelength matched with the Soret band (maximum absorption peak) of photosensitizers (for porphyrin analogues, it locates around 400 nm) has attracted many researchers. In theory, laser wavelength matched with the maximum absorption peak of photosensitizer can excite the photosensitizer with maximal efficacy. However, it is not the fact that *in vivo*, as other factors (such as light peneration and distribution in tissue) can also dimensionally affect the intensity of PDT reaction. Our previous theoretical simulation showed that as the backscattering of 413 nm is bigger than that of 532 nm, it can only penetrate into the shallow vessels in PWS, and the light distribution and singlet oxygen generated at 413 nm in vessels are not as uniform as that at 532 nm. It suggested that 413 nm might be the suitable wavelength for pediatric PWS patients whose epidermis is thinner and more transparent than adults, while not for adult patients or higher grade patients. The clinical work of the Laser Centre of Shanghai Ninth People's Hospital in China made by Krypton laser at 413 nm also verified it.[18]

Therefore, the mathematical simulation in this study is very useful to enhance our understanding of the fundamental processes in PDT and to help us improve the treatment outcomes. The simulation results suggested that besides the excitation efficiency of photosensitizer at different laser wavelengths, the selective distribution of laser in ectatic vessels of PWS is another key factor in determining the selective destruction of target vessels. A laser wavelength that penetrates too deep (such as 630 nm) or too shallow in PWS skin is not appropriate for PDT for PWS. Because in the first situation, PDT would lead to damage of the dermis, which may result in scars, and there will not be enough damage to the ectatic vessels in the second situation. The simulation results indicated that individualization of PDT dosimetry can be obtained by adopting various laser wavelengths according to the age, skin color of each patient, and the morphosis of PWS vessels. Apart from the generally used 532 nm laser PDT in clinic, a short wavelength such as 413 nm is suitable to pediatric patients and a 510 nm can be applied to the treatment of deeply located PWS vessels or PWS with hyperpigmentation skin.

Furthermore, this theoretical simulation can help us investigate which wavelength would be the most advantageous to be used in PDT for PWS. According to the results of this study, the optimal wavelength should near the absorption peaks of photosensitizer and near the wavelengths where absorption from native chromophores (haemoglobin and melanin) is diminished. For the present available porphyrin analogous photosensitizer in clinic, a wavelength around 500 nm is a good light source. For PWS in which the superficial vessels have been cleared in the previous treatments and PWS with hyperpigmentation after previous PDT, satisfactory therapeutic result can still be obtained by using a 510 nm laser. In these PWS, it is usually difficult to get a good therapeutic result by 532 nm PDT. Although no light source at present is available for PDT around 500 nm wavelength besides the large copper vapor laser, due to the rapid development of new high-power laser, it is very likely that PDT light sources at these wavelengths will be developed in coming years. Moreover, many new photosensitizers for V-PDT were synthetized and studied in recent years. With a theoretical study such as this, we can investigate which wavelength would be the optimal PDT light source for a certain photosensitizer.

Appendix

The calculation of optical property parameters at different wavelengths is described as follows:

$$\begin{bmatrix} u_a \\ u_s \\ g \\ n \end{bmatrix} = \begin{bmatrix} u_a^1 & u_a^2 \\ u_s^1 & u_s^2 \\ g^1 & g^2 \\ n^1 & n^2 \end{bmatrix} \times \begin{bmatrix} f_1 \\ f_2 \end{bmatrix}. \tag{8}$$

For example, the total optical absorption coefficient of the epidermis or dermis is

$$\mu_{\mathrm{a}} = f_{\mathrm{chrom}} \cdot \mu_{\mathrm{a,chrom}} + (1 - f_{\mathrm{chrom}})\mu_{\mathrm{a,base}}, \tag{9}$$

where f_{chrom} is the volume fraction of melanin in the basal layer of the epidermis or volume fraction of blood in dermis, $\mu_{\mathrm{a,chrom}}$ (cm^{-1}) is the absorption coefficient of melanin or blood. $\mu_{\mathrm{a,base}}$ is the absorption coefficient of the epidermis with less melanin or dermis without ectatic vessels. The absorption coefficient and scattering coefficients of melanin, blood, and epidermis with less melanin and dermis without ectatic vessels were chosen from the compiled data of Jacques.[19]

$$\mu_{a,mel} = 6.6 \times 10^{11} \cdot \lambda^{-3.33}. \tag{10}$$

The total optical scattering coefficient of the epidermis or dermis is calculated according to the above method. The values

of g for each wavelength were chosen from the literature of van Gemert.[20]

Acknowledgments

This project was supported by the National Natural Science Foundation of China (Nos. 60878055 and 61036014) and the National 863 Research Project of China (Nos. 2007AA04Z231 and 2008AA0301171).

References

1. S. H. Barsky, S. Rosen, D. E. Geer, and J. M. Noe, "The nature and evolution of port wine stains: a computer-assisted study," *J. Invest. Dermatol.* **74**, 154–157 (1980).
2. R. R. Anderson and J. A. Parrish, "Selective photothermolysis: precise micro-surgery by selective absorption of pulsed radiation," *Science* **220**, 524–527 (1983).
3. J. M. Smit, C. G. Bauland, D. S. Wijnberg, and P. H. M. Spauwen, "Pulsed dye laser treatment, a review of indications and outcome based on published trials," *Br. J. Plast. Surg.* **58**(7), 981–987 (2005).
4. Y. Gu, J. H. Li, Y. P. Jiang, J. Liang, P. Zhou, X. J. Cui, Y. M. Pan, and K. Wang, "A clinical study of photodynamic therapy for port wine stain," *Chin. J. Laser Med. Surg.* **1**(1), 6–10 (1992).
5. R. Tao, Y. Gu, F. G. Liu, J. Zeng, L. Zhang, and Y. M. Pan, "Mechanism of photosensitizerd reaction induced by Hematoporphyrin Monomethyl Ether in vitro," *Chin. J. Laser Med. Surg.* **11**(3), 149–153 (2002).
6. Y. Wang, X. H. Liao, and Y. Gu, "Preliminary study on oxygen content monitoring for port wine stains during PDT using diffuse reflection spectra," *Guang Pu Xue Yu Guang Pu Fen Xi* **30**(12), 3363–3366 (2010).
7. Y. Wang, X. H. Liao, and Y. Gu, "Fluorescence monitoring of a photosensitizer and prediction of the therapeutic effect of photodynamic therapy for port wine stains," *Exp. Biol. Med.* **235**, 175–180 (2010).
8. Y. Gu, F. G. Liu, K. Wang, J. G. Zhu, J. Liang, Y. M. Pan, and J. H. Li, "A clinic analysis of 1216 cases of port wine stain treated by photodynamic therapy," *Chin. J. Laser Med. Surg.* **10**(2), 86–89 (2001).
9. Y. Gu, J. H. Li, H. Y. Shan, K. Wang, Y. P. Jiang, Y. Zhang, J. Liang, Y. M. Pan, Z. Z. Yu, J. Y. Zhang, G. Liu, Y. Z. Tu, and L. Ren, "Clinical Application of Copper Vapor Laser in PDT for Fifty Cases of PWS," *Chin. J. Laser Med. Surg.* **3**(4), 215–217 (1994).
10. G. Cheng, Q. H. Zhong, F. G. Liu, and N.Y. Huang, "Modeling and simulation of the acting factors on vascular selectivity of photodynamic therapy," *Chin. J. Lasers.* **32**(6), 864–868 (2005).
11. Y. Wang, Y. Gu, R. Chen, L. Q. Xu, X. H. Liao, N. Y. Huang, and Y. Y. Wang, "Comparison between HMME mediated photodynamic therapy using 413 nm and 532 nm for port wine stains – a mathematical simulation study," *Proc. SPIE* **6826**, 68261L (2007).
12. T. Dai, B. M. Pikkula, L. V. Wang, and B. Anvari, "Comparison of human skin opto-thermal response to near-infrared and visible laser irradiations: a theoretical investigation," *Phys. Med. Biol.* **49**, 4861–4877 (2004).
13. L. O. Svaasand, P. Wyss, M. T. Wyss, Y. Tadir, B. J. Tromberg, and M. W. Berns, "Dosimetry model for photodynamic therapy with topically administered photosensitizers," *Lasers Surg. Med.* **18**,139–149 (1996).
14. M. G. Nichols and T. H. Foster, "Oxygen diffusion and reaction kinetics in the photodynamic therapy of multicell tumour speroids," *Phys. Med. Biol.* **39**, 2161–2181 (1994).
15. I. Georgakoudi, M. B. Nichols, and T. H. Foster, "The mechanism of photofrin photobleaching and its consequences for photodynamic dosimetry," *Photochem. Photobiol.* **65**, 135–144 (1997).
16. T. H. Foster, R. S. Murant, R. G. Bryant, R. S. Knox, S. L. Gibson, and R. Hilf, "Oxygen consumption and diffusion effects in photodynamic therapy," *Radiat. Res.* **126**, 296–303 (1991).
17. A. Blum and L. I. Grossweiner, "Singlet oxygen generation by hematoporphyrin IX uroporphyrin I and hematoporphyrin derivative at 546 nm in phosphate buffer and in the presence of egg phosphatidylcholing liposomes," *Photochem. Photobiol.* **41**, 27–32 (1985).
18. G. Y. Zhou and Z. Y. Zhang, "Preliminary clinical study on krypton laser photodynamic therapy for PWS," *Shanghai J. Stomatology* **9**(3), 168–170 (2000).
19. S. L. Jacques, *Skin Optics*, Oregon Medical Laser Center News, Jan 1998, http://omlc.ogi.edu/news/jan98/skinoptics.html.
20. M. J. C. van Gemert, S. L. Jacques, H. J. C. M. Sterenborg, and W. M. Star, "Skin Optics," *IEEE Trans. Biomed. Eng.* **36**, 1146–1154 (1989).